

PETAR D. JANJATOVIĆ <sup>1</sup>  
OLIVERA A. ERIĆ CEKIĆ <sup>2,3</sup>  
DRAGAN M. RAJNOVIĆ <sup>1</sup>  
SEBASTIAN S. BALOŠ <sup>1</sup>  
VENCISLAV K. GRABULOV <sup>4</sup>  
LEPOSAVA P. ŠIDJANIN <sup>1</sup>

<sup>1</sup> Department of Production  
Engineering, Faculty of  
Technical Science, University of  
Novi Sad, Novi Sad, Serbia

<sup>2</sup> Innovation Center of Mechanical  
Engineering Faculty, University of  
Belgrade, Belgrade, Serbia

<sup>3</sup> Faculty of Mechanical and Civil  
Engineering, University of  
Kragujevac, Kraljevo, Serbia

<sup>4</sup> Institute for testing of  
materials-IMS, Belgrade, Serbia

SCIENTIFIC PAPER

UDC 669.13:621.74:620

## MICROSTRUCTURE AND FRACTURE MODE OF UNALLOYED DUAL-PHASE AUSTEMPERED DUCTILE IRON

### Article Highlights

- Dual-phase ADI provides a range of properties due to free ferrite and ausferrite constituents
- With the increase in austenitization temperature, a higher amount of ausferrite is formed
- Specimens with the highest values of ausferrite have a dominant quasi-cleavage type of fracture
- Quasi-cleavage fracture around last-to-freeze zones is related to the presence of ausferrite
- Ausferrite influences the rise in strength and the drop in ductility

### Abstract

*Dual-phase ADI material microstructure consists of different amounts and morphologies of ausferrite and free ferrite, obtained by subjecting ductile iron to specific heat treatment. Its strength is lower compared to comparable ADI materials but exhibits a higher ductility, the major disadvantage of ADI. In the current study, an unalloyed ductile iron was intercritical austenitized in two-phase regions ( $\alpha+\gamma$ ) at four temperatures from 840 to 780 °C for 2 h and austempered at 400 °C for 1 h to obtain dual-phase ADI with different percentages of free ferrite and ausferrite. Light and scanning electron microscopy was performed for the metallographic and fracture studies, respectively. Microscopy results were correlated to tensile testing results. The results indicated that, as the amount of ausferrite present in the matrix increases, higher values of strength and lower ductility are obtained. The fracture surfaces of dual-phase ADI microstructures with 22.8% of ausferrite in their matrix have regions of quasi-cleavage fracture around last-to-freeze zones, related to the presence of ausferrite in those areas. The specimens with the highest values of ausferrite of 86.8% among the dual-phase microstructure have a dominant quasi-cleavage type of fracture.*

*Keywords:* dual matrix structure, austempered ductile iron, microstructure, surface of fracture.

Austempered ductile iron (ADI) is an isothermally modified ductile cast iron with a unique ausferritic microstructure consisting of ausferritic ferrite and carbon enriched retained austenite, and it is free of carbides. This microstructure, combined with spherical graphite, provides relatively high tensile properties, similar to heat-treated steels, with a lower density and

significantly lower fabricating costs. These properties make the ADI materials very attractive today, particularly for manufacturing parts in automotive, agricultural, railroad, mining, and other heavy industry sectors. Particular attention has been paid to tensile properties, wear, cavitation, and even ballistic properties of ADI materials [1-3]. In recent years, a new type of ductile cast iron material, called “dual-phase austempered ductile iron” (dual-phase ADI), has become an active field of research and development [4]. The microstructure of the dual-phase ADI matrix consists of different amounts and morphologies of ausferrite (common ADI microstructure) and free (proeutectoid or allotriomorphic) ferrite, which is obtained by subjecting ductile iron to specific heat treat-

Correspondence: O.A. Erić Cekić, Faculty of Mechanical and Civil Engineering, University of Kragujevac, Kraljevo, Serbia.  
E-mail: [olivera66eric@gmail.com](mailto:olivera66eric@gmail.com)  
Paper received: 22 December, 2020.  
Paper revised: 27 April, 2021.  
Paper accepted: 23 July, 2021.

<https://doi.org/10.2298/CICEQ201222027J>

ments.

This dual-phase microstructure is obtained by intercritical annealing (partial austenitization) in the ( $\alpha$ + $\gamma$ +graphite) region, whereby colonies of free ferrite are introduced. Partial austenitization is finally followed by austempering in the conventional temperature range 250–400 °C up to several hours. As a result, depending on the temperature of austenitization, the matrix of the dual-phase ADI contains different amounts of free ferrite (FF) and ausferrite (AF). Compared to the conventional ductile irons, the ADI with dual-phase microstructure obtained has a higher ratio of strength to ductility [5]. The selections of different intercritical temperatures make it possible to get different combinations of free ferrite to ausferrite percentages.

Mechanical properties of the dual-phase ADI depend on the volume amount of free ferrite and the amount and morphology of ausferrite, which, in turn, is a function of the intercritical austenitizing temperature selected and an austempering treatment, as aforesaid [6-9]. Additionally, the dual-phase ADI could provide a wide range of mechanical properties as a function of the relative proportion of free ferrite and ausferrite microconstituents, thereby replacing standard ductile iron and austempered ductile iron in different applications [10]. Aranzabal *et al.* [11] studied the new mixed (ferritic-ausferritic) ductile iron for automotive suspension parts. It was found that the yield stress and tensile strength values of dual-phase ADI, together with its hardness, are similar to those of fully pearlitic ductile irons. In contrast, ductility remains at the same level as in ferritic ductile irons.

Recently, it has been shown by Wade and Ueda [12] and Verdu *et al.* [13] that the mechanical properties (yield stress, tensile strength, and hardness) of dual-phase ADI austempered at 375 °C increases as the ausferrite volume fraction in the microstructure of free ferrite and graphite nodules increase. Works carried out by Kilicli and Erdogan [9,10] were focused on the dual-phase ADI mechanical properties, particularly for those austempered at 365 °C and a wide variety of ferrite-ausferrite combinations. An interesting result was for the 45% ausferrite and 65% ferrite microstructure that yielded the most convenient strength-toughness ratio.

The fracture surfaces of the dual-phase ADI with different amounts of ferrite-ausferrite were also evaluated by several authors [14,15]. Nevertheless, there is no complete understanding of the sequence and occurrence of damage mechanisms, the influence of the morphology and ausferrite volume fraction on crack propagation, and damage evolution. In most

publications [15-20], the study of the fracture surface, obtained by tensile tests of ADI with dual matrix structure with different amounts of ferrite-ausferrite, has been relatively brief. In general, studies of the dual-phase ADI have focused on studying the role of different microconstituents during fatigue and tensile testing using in-situ analysis [19-22]. In the literature, very little information is currently available about the influence of the different amounts of the free ferrite and the ausferrite volume fractions and their distribution on the morphology of the fracture surfaces of dual-phase ADI [5-9].

This study aims to evaluate the fracture surfaces obtained using tensile tests from different samples of dual-phase ADI. The main objective of this work is to study the tensile fracture behavior of dual-phase ADI and ductile cast iron with a microstructure consisting of spherical graphite in a predominantly ferrite matrix with 10% pearlite and correlate the observed fracture mode and the tensile properties obtained.

## MATERIALS AND METHODS

### Materials

The material used in this study was industrially produced ductile iron keel blocks obtained in a commercial electro-induction foundry furnace. The melt was poured from about 1420 °C into a standard 25.4 mm Y block sand mold (ASTM A-395), ensuring sound castings. The chemical composition was determined on white cast samples using optical emission spectroscopy on ARL-2460. Tensile specimens with 6 mm diameter and 30 mm gauge length were machined from Y blocks.

The methodology employed to establish the heat treatment used to obtain "dual-phase" austempered ductile iron microstructures was determined according to the procedure described in previous papers by the authors [7-8]. An austempering temperature of 400 °C was selected to obtain a higher ductility of the ausferrite and thus higher ductility of dual-phase austempered ductile iron [2-6].

Heat treatment (HTA) of tensile specimens consisted of austenitization within the intercritical interval at 780, 800, 820, and 840 °C for 2 h, followed by austempering at 400 °C for 1 h in all cases. The obtained samples have been designated HTA-1, HTA-2, HTA-3, and HTA-4.

### Methods

#### *Metallurgical evaluation*

Standard metallographic preparation techniques

(mechanical grinding and polishing, followed by etching in Nital) were applied before light microscopy (LM) examinations on an Orthoplan microscope (Leitz, Germany). The relationship between the amount (% in volume) of free ferrite (FF), ausferrite (AF), and graphite (Gr) in dual-phase ADI microstructures was quantified by image analysis software JMicroVision. The reported values average at least five analyzed fields of view on each sample.

#### Hardness measurement

The Vickers hardness HV10 (ISO 6507) was determined with a test load of 98.07 N (10 kg) and a dwell time of 15 s. The testing machine was an HPO 250 (WPM, Germany).

#### Tensile test

The specimens' tensile tests were performed on a WPM ZDM 5/91 (WPM, Germany) tensile testing machine equipped with an S-type measuring tension force sensor and linear variable differential transformer LVDT inductive sensor (HBM Germany). A Spider 8 (HBM, Germany) acquisition device connected the sensors to a PC. The tensile tests were done according to ISO 6892. The 0.2% proof stress (PS), the ultimate tensile stress (UTS), and elongation at failure (A) were measured.

The fractured surfaces of tensile-tested specimens were examined by a scanning electron microscope JEOL JSM 6460LV (JEOL, Japan) operated at 25 kV.

## RESULTS AND DISCUSSION

### Chemical composition and microstructures

The chemical composition of the as-cast ductile iron melt is shown in Table 1.

Table 1. The chemical composition of as-cast ductile iron

C	Si	Mn	Ni	Cr	Mg	P	S	Fe
3.5	2.5	0.35	0.05	0.06	0.031	0.018	0.015	balance

The microstructure of samples in as cast condition reflected that the original matrix was over 90% ferritic, with a nodularity of over 90%, an average nodule size of 20  $\mu\text{m}$ , and an average nodule distribution of about 150 per  $\text{mm}^2$ , according to the ASTM A247 standard. Figure 1 illustrates the overall microstructure appearance obtained for all specimens austenitized at different temperatures within the intercritical interval (austenitizing temperatures employed were 780  $^{\circ}\text{C}$ , 800  $^{\circ}\text{C}$ , 820  $^{\circ}\text{C}$ , and 840  $^{\circ}\text{C}$ ) and austempered in the salt bath at 400  $^{\circ}\text{C}$  during 1 h. The different intercritical austenitization temperatures

allowed the microstructure to attain various amounts of ausferrite (AF) and free ferrite (FF). As shown in Figure 1, the amount of FF and AF directly depends on the austenitizing temperature. At lower austenitization temperatures (Figure 1a), there is a lower percentage of the AF, which is increased as the austenitization temperature increases (Figure 1d), and vice versa in the case of the FF. The relative amount of free ferrite (FF) decreases with the increase of austenitization temperature from 65.2 to 2%, while the amount of ausferrite (AF) increases from 22.8 to 86.8% (see Table 2). The dual-phase ADI microstructure achieved after austenitizing closer to the upper critical temperature (Figure 1d) consists almost entirely of ausferrite.

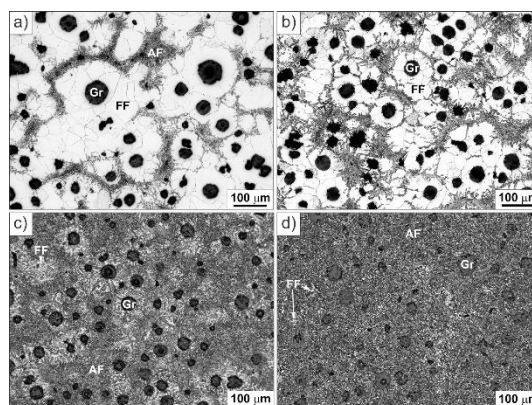


Figure 1. The amount of phases in samples austenitized at different austenitisation temperatures  $T_v$ : a)  $T_v = 780\text{ }^{\circ}\text{C}$ ; 65.2%FF+22.8%AF+12%Gr, b)  $T_v = 800\text{ }^{\circ}\text{C}$ ; 42.8%FF+42.4%AF+14.8%Gr, c)  $T_v = 820\text{ }^{\circ}\text{C}$ ; 8%FF+80%AF+12%Gr, d)  $T_v = 840\text{ }^{\circ}\text{C}$ ; 2%FF+86.8%AF+11.2%Gr; FF (free ferrite), AF (ausferrite), Gr (graphite nodule).

Observation under higher magnification reveals different morphologies of microstructures present in the dual-phase ADI samples, Figure 2. The phases are easily distinguishable, as the free ferrite (FF) has a flat white surface, and retained austenite (RA) is more oblique with a more pronounced boundary (bevel edge). Also, RA has a more grayish appearance compared to FF. The ausferritic ferrite (AAF) plates in retained austenite (RA) could be recognized by gray to dark shade tinting.

The size of ausferritic ferrite plates changes with austenitization temperature, primarily due to the amount and size of prior austenite grains produced at different austenitization temperatures. At lower austenitization temperatures (780  $^{\circ}\text{C}$ ), the prior-austenite grains are smaller, confined by the larger amount of free ferrite. Thus, the formed ausferrite ferrite plates during subsequent austempering are shorter and more randomly oriented (Figure 2a). With the increase of austenitization temperature (800 and 820  $^{\circ}\text{C}$ ), the amount of ausferrite increases due to the formation of

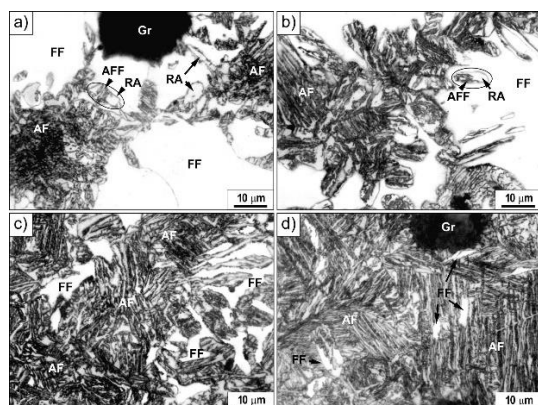


Figure 2. Microstructure of samples austenitised at different austenitisation temperatures  $T_A$ : a)  $T_A = 780$  °C; b)  $T_A = 800$  °C; c)  $T_A = 820$  °C d)  $T_A = 840$  °C; FF (free ferrite), AF (ausferrite), Gr (graphite nodule), RA (retained austenite), AFF (ausferritic ferrite).

a higher amount of austenite of larger grain size (Figure 2b and c). In this case, ausferritic ferrite plates grow more easily, resulting in more elongated AFF plates and thus a more acicular appearance of ausferrite (AF). At austenitization temperatures of 840 °C, the microstructure is dominantly austenitic, which upon quenching to austempering temperature, freely can transform to ausferrite (Figure 2d). Produced ausferrite has long ausferritic ferrite plates, similar to acicular microstructure, which might be observed in conventional ADI material.

The width of ausferritic ferrite plates does not change significantly with increasing austenitization temperature. Although, more different sizes (larger spread) could be noticed at lower temperatures due to smaller prior-austenite grain size and faster austempering transformation.

### Mechanical properties

The results of mechanical properties, depending on the amount of microconstituents in the samples used in this study, are given in Table 2.

It can be seen that the amount of ausferrite increases in dual-phase- ADI, ultimate tensile strength (UTS), proof strength (PS), and hardness (HV10) increases also. An increase in the amount of ausferrite in the matrix promotes higher values of the UTS and PS up to a peak value of 917 MPa and 720 MPa, respectively. This corresponds to the sample composed of 80% ausferrite and 8% free ferrite. The value of elongation (A) has an opposite trend. The lowest elongation values are correlated with the maximum values of ausferrite.

### Fracture mode

The fracture surfaces of tensile test specimens were analyzed by SEM. The failure regions in the as-cast, mostly ferritic specimen, exhibit a uniform distribution of graphite nodules (Figure 3). Furthermore, there is a high degree of deformation around the graphite nodules. In addition, the ferritic space between nodules undergoes a substantial plastic deformation exhibiting dimples (Figure 3b). The fracture surface contains a relatively larger cavity size than the graphite nodule size (Figure 3b). Formation of the cavity may be attributed to decohesion at the graphite and surrounding ferrite matrix. The dimple pattern around the graphite nodules shows the deformation of the surrounding ferrite matrix during the final period of straining up to fracture. Voids characterize a typical fracture mode of ductile iron in its microstructure and a result of nodular cavities and possible the last-to-freeze (LTF) zones generated during solidification [23,24]. The appearance of last-to-freeze (LTF) regions are deliberated weak areas within the metallic matrix, and typical casting defects such as inclusions, porosity, and microshrinkage are present in these regions [23,24].

The SEM micro-fractographs of the dual-phase ADI samples, containing 22.8%, 42.4%, 80%, and 86.8% of ausferrite in the microstructure, are shown in Figure 4. The appearance of the dimpled fracture zone

Table 2. The mechanical properties and microconstituents percentages of as-cast ductile cast iron and dual-phase ADI alloys

Material	Proof strength	Ultimate tensile strength	Elongation	Ausferrite	Free Ferrite	Hardness
	PS [MPa]	UTS [MPa]	A [%]	vol. fraction	vol. fraction	HV10
As-cast ductile iron	318	456	19.1	/	/	150
HTA-1:(780 °C-2h/400 °C-1h)	340	478	16.0	22.8	65.2	164
HTA-2:(800 °C-2h/400 °C-1h)	395	557	12.8	42.4	42.8	202
HTA-3:(820 °C-2h/400 °C-1h)	620	825	11.7	80.0	8.0	296
HTA-4:(840 °C-2h/400 °C-1h)	709	915	11.0	86.8	2.0	292

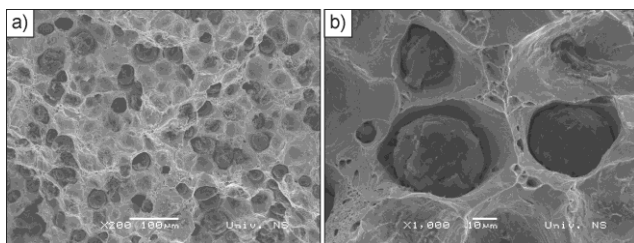


Figure 3. SEM fracture surface of as-cast ductile iron after failure in tension test: a) dimpled fracture surface, b) graphite nodules that undergone decohesion from the metal matrix.

in all specimens reveals a ductile (DF), quasi-cleavage (QCF), and brittle fracture (BF). A somewhat higher number of dimples with a cleavage facet was observed in the specimen with 42.4% ausferrite, Figure 4b. Ferrite volume fraction or ausferrite may play an essential role in determining fracture mode since ferrite fails in a more ductile mode and its contribution to the fracture resistance increases with increasing ferrite volume fraction. The quasi-cleavage pattern of fracture of the specimen with a higher ausferrite or low ferrite volume fraction, the majority of the fracture surface shows a quasi-cleavage pattern of fracture, reflecting the low ductility and fracture energy of this material. These findings are in agreement with the previously published results [14,15,18].

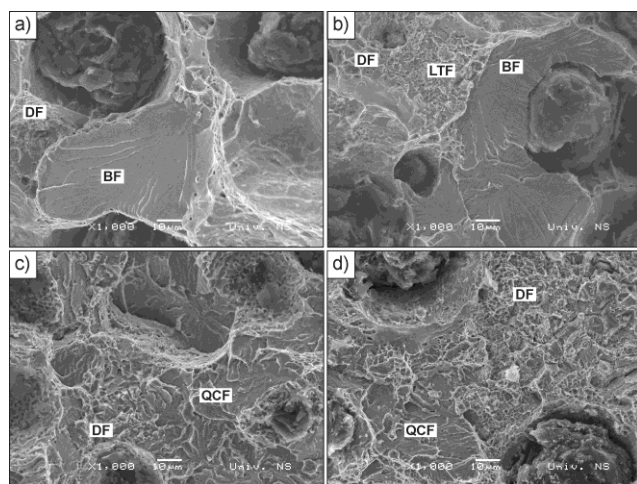


Figure 4. The fracture surfaces for specimens austenitised at: a)  $T_r = 780\text{ }^\circ\text{C}$  (22.8% AF), b)  $T_r = 800\text{ }^\circ\text{C}$  (42.4% AF), c)  $T_r = 820\text{ }^\circ\text{C}$  (80% AF), d)  $T_r = 840\text{ }^\circ\text{C}$  (86.8% AF); DF (ductile fracture), BF (brittle fracture), QCF (quasi-cleavage fracture), LTF (last to freeze zone).

In Figure 4c, the fracture surface of the specimen containing 80% ausferrite in the matrix is shown. A higher amount of ausferrite in the matrix produced a flat fracture surface, closely related to quasi-cleavage fracture mechanics [15,25,26].

The micrographs of specimens with highest values of ausferrite of 86.8% among the dual-phase

structure, the dominant form of the fracture surface was a quasi-cleavage type, Figure 4d.

The increased amount of ausferrite in the matrix (as shown in Figures 4a-d) increases the tendency to exhibit quasi-cleavage fracture. It is important to note the increase of ausferrite volume fraction in the matrix produced a reduced brittle fracture zone while that of the ductile fracture pattern and quasi-cleavage increased. The brittle fracture is observed in the specimens with 22.8% ausferrite (Figure 4a) near the graphite nodules. In comparison, the fully quasi-cleavage fracture is present for the high amounts of ausferrite in the specimen (HTA-4) with 86.8% of ausferrite (Figure 4d).

It is well documented [14,15] that in the dual-phase microstructure, the high strength ausferrite may restrict the deformation of low strength ferrite under tensile loading. The ductility decreases with increasing continuity of the ausferrite structure along eutectic cell boundaries. This may be explained considering that the high strength ausferrite may restrict the deformation of low strength ferrite under tensile loading at the moment of fracture. In this case, the low-strength ferrite in the rest of the matrix will be plastically deformed until the moment when the ausferrite breaks. It is reasonable to accept that at that moment, the higher strength of the ausferrite suffered by the ausferrite is suddenly transferred on the matrix of free ferrite, and a rapid fracture with a brittle appearance occurs.

As expected, the fracture in the case of a larger amount of free ferrite has a more brittle appearance (although the fracture strength is lower, and the ductility of the whole sample is higher). In comparison, we have standardly observed ductile and quasi-cleavage fracture in the case of a larger amount of ausferrite.

## CONCLUSION

Based on test results and their analysis, the following conclusions can be summarized as:

The fracture mode of the specimen having predominantly ferritic matrix is ductile as characterized by microvoid coalescence and dimple rupture phenomena. The change of fracture mechanism could be correlated to a change in elongation and the relative proportion of free ferrite and ausferrite constituents in dual-phase ADI microstructure. The fracture surfaces of dual-phase ADI microstructures with 22.8% of ausferrite in their matrix have regions of quasi-cleavage fracture around last-to-freeze zones, related to the presence of ausferrite in those areas. The decrease in nodular cavities deformation and a higher amount of quasi-cleavage zones is a consequence of the increase

of volume fractions of ausferrite in dual-phase ADI microstructure. The specimens with the highest values of ausferrite of 86.8% among the dual-phase microstructure have a dominant quasi-cleavage type of fracture. Ausferrite represents a crucial phase in the metal matrix that influences the rise in strength and the drop in ductility. It can be regarded as one of the decisive influencing factors on the applicability of ADI, including dual-phase ADI.

### Acknowledgment

This paper has been supported by the Ministry of Education, Science and Technological Development of the Republic of Serbia through project no. 451-03-68/2020-14/200156: “Innovative scientific and artistic research from the Faculty of Technical Sciences, Novi Sad, Serbia, activity domain” and project no. 451-03-68/2020-14/200213, Innovation Centre of Mechanical Engineering Faculty, University of Belgrade, Belgrade, Serbia.

The support has also been received from the Materials testing laboratory, Department of Production Engineering, Faculty of Technical Sciences Novi Sad Serbia, within the framework of the project entitled “Innovative materials and joining technologies.”

### REFERENCES

- [1] W. Bingxu, Q. Feng, C. Gary, Barber, P. Yuming, C. Weiwei, W. Rui, *J. Mater. Res. Technol.* 9 (5) (2020) 9838-9855.
- [2] P. Janjatovic, O. Eric Cekic, L. Sidjanin, S. Balos, M. Dramicanin, J. Grbovic Novakovic, D. Rajnovic, *Met.* 11 (2021) 1-16.
- [3] S. Balos, I. Radisavljevic, D. Rajnovic, P. Janjatovic, M. Dramicanin, O. Eric- Cekic, L. Sidjanin, *Def. Sci. J.* 69 (2019), 571-576.
- [4] A. Basso, J. Sikora, *Int. J. Metalcast.* 6 (2012) 1-14.
- [5] R. Steiner, in *ASM Handbook Vol. 1*, by ASTM International, Ohio, USA, 33 (1990), p. 1005.
- [6] C. Verdu, J. Adrien, A. Reynaud, *Int. J. Cast Met. Res.* 18 (2005) 346-354.
- [7] A. Basso, R. Martinez, J. Sikora, *Mater. Sci. Technol.* 23 (2007) 1321-1326.
- [8] A. Basso, R. Martinez, J. Sikora, *Mater. Sci. Technol.* 25 (2008) 1271-1278.
- [9] V. Kilicli, M. Erdogan, *Mater. Sci. Technol.* 22 (2006) 919-928.
- [10] V. Kilicli, M. Erdogan, *Int. J. Cast. Met.* 20 (2007) 202-214.
- [11] J. Aranzabal, G. Serramoglia, D. Rousiere, *Int. J. Cast Met. Res.* 16 (2002) 185-190.
- [12] N. Wade, Y. Ueda, *Trans. ISII*, 21 (1981) 117-126.
- [13] C. Verdu, J. Adrien, A. Reynaud, *Int. J. Cast. Met. Res.* 18 (2005) 346-354.
- [14] A. Basso, J. Sikora, R. Martínez, *Fatigue Fract. Eng. Mater. Struct.* 36 (7) (2013) 650-659.
- [15] V. Kilicli, M. Erdogan, *J. Mater. Eng. Perform.* 19 (2010) 142-149.
- [16] F. Iacoviello, V. Di Cocco, M. Cavallini, *Fatigue Fract. Eng. Mater. Struct.* 39 (2016) 999-1011.
- [17] F. Iacoviello, V. Di Cocco, A. Rossi, M. Cavallini, *Fratt. Integrita Strutt.* 7 (25) (2013) 102-108.
- [18] L. D'Agostino, V. Di Cocco, O. Fernandez, D. F. Iacoviello, *Process. Struct. Integr.* 3 (2017) 201-207.
- [19] D.O. Fernandez, R.E Boeri, *Fatigue Fract. Eng. Mater. Struct.* 42 (2019) 2220-2231.
- [20] R.C. Voigt, L.M. Elderly, H.S. Chiou, *AFS Trans.* 94 (1986) 645-656.
- [21] T. Kobayashi, S. Yamada, *Metall. Mat. Trans. A* 27 (1996) 1961-1971.
- [22] A. Basso, M. Caldera, M. Chapetti, J. Sikora, *ISIJ, Int.* 50 (2010) 302-306.
- [23] R. Voigt, L. Eldoky, *AFS Trans.* 94 (1986) 645-656.
- [24] R. Martínez, R. Boeri, J. Sikora, *Jornadas SAM Asociación Argentina de Materiales - IV Latin-American Colloquium on Fracture and Fatigue, Neuquen, Argentina (2000) p.615.*
- [25] L. Masud, R. Martinez, S. Simison, R. Boeri, *J. Mater. Sci.* 38 (2003) 2971-2977.
- [26] R. Martinez, *Eng. Fract. Mech.* 77 (2010) 2749-2762.

PETAR D. JANJATOVIĆ <sup>1</sup>  
OLIVERA A. ERIĆ CEKIĆ <sup>2,3</sup>  
DRAGAN M. RAJNOVIĆ <sup>1</sup>  
SEBASTIAN S. BALOŠ <sup>1</sup>  
VENCISLAV K. GRABULOV <sup>4</sup>  
LEPOSAVA P. ŠIDJANIN <sup>1</sup>

<sup>1</sup> Departman za proizvodno  
mašinstvo, Fakultet tehničkih  
nauka, Univerzitet u Novom  
Sadu, Novi Sad, Srbija

<sup>2</sup> Inovacioni centar mašinskog  
fakulteta u Beogradu, Univerzitet  
u Beogradu, Beograd, Srbija

<sup>3</sup> Fakultet za mašinstvo i  
građevinarstvo u Kraljevu,  
Univerzitet u Kragujevcu,  
Kraljevo, Srbija

<sup>4</sup> Institut za ispitivanje  
materijala IMS, Beograd, Srbija

## MIKROSTRUKTURA I MORFOLOGIJA LOMA NELEGIRANOG DVOFAZNOG AUSTEMPEROVANOG NODULARNOG LIVA

*Mikrostruktura dvofaznog austemperovanog nodularnog liva proizvedena je specifičnom termičkom obradom nodularnog liva i sastoji se od različitih količina i morfologije ausferita i slobodnog ferita. Zahvaljujući takvoj mikrostrukturi dvofazni austemperovani nodularni liv ima nižu vrednost čvrstoće u poređenju sa konvencionalnim ADI materijalima, ali veću duktilnost. U ovoj studiji, nelegirani nodularni liv je bio austenitizovan u međukritičnom dvofaznom području ( $\alpha+\gamma$ ) na četiri temperature od 780 do 840 °C tokom 2 sata i zatim austemperovan na 400 °C tokom 1 sata da bi se dobio dvofazni ADI sa različitim procentima slobodnog ferita i ausferita. Metalografska analiza i analiza morfologije loma izvršena su pomoću svetlosnog i skenirajućeg elektronskog mikroskopa, respektivno. Rezultati mikroskopije su upoređeni sa rezultatima ispitivanja zatezanjem. Rezultati ukazuju da se sa povećanjem količine ausferita prisutnog u osnovi postižu veće vrednosti čvrstoće, ali i manja duktilnost. Površina loma dvofaznih ADI materijala sa 22,8% ausferita u osnovi sastoji se iz područja loma nastalog mehanizmom kvazi-cepanja oko zona koje su poslednje očvrsle, što se može povezati sa prisustvom ausferita u tim oblastima. Uzorci sa najvećom vrednošću ausferita od 86,8% u dvofaznoj mikrostrukturi imaju dominantan lom nastao mehanizmom kvazi-cepanja.*

*Ključne reči: dvofazna struktura, austemperovani nodularni liv, mikrostruktura, prelom.*

NAUČNI RAD